

Interference-filter-stabilized external-cavity diode lasers

X. Baillard, A. Gauguet, S. Bize, P. Lemonde, Ph. Laurent,
A. Clairon, P. Rosenbusch

Systèmes de Référence Temps-Espace, Observatoire de Paris,
61 avenue de l'Observatoire, 75014 Paris, FRANCE*

Abstract

We have developed external-cavity diode lasers, where the wavelength selection is assured by a low loss interference filter instead of the common diffraction grating. The filter allows a linear cavity design reducing the sensitivity of the wavelength and the external cavity feedback against misalignment. By separating the feedback and wavelength selection functions, both can be optimized independently leading to an increased tunability of the laser. The design is employed for the generation of laser light at 698, 780 and 852 nm. Its characteristics make it a well suited candidate for space-born lasers.

Key words: external cavity laser, interference filter, grating, stability, tunability, laser cooling

PACS: 42.55.-f

1 Introduction

Semiconductor lasers have become an inexpensive easy-to-handle source of coherent light. Applications in many fields such as atomic physics, metrology and telecommunication require single mode operation with narrow linewidth and good tunability [1]. This is frequently achieved by incorporating the laser diode into an external cavity where optical feedback and wavelength discrimination are provided by a diffraction grating [2]. However, such a design is sensitive to the ambient pressure [3] and to optical misalignment [4] induced by mechanical or thermal deformation. In addition, for the common Littrow configuration,

Email address: Peter.Rosenbusch@obspm.fr.

URL: opdaf1.obspm.fr.

the direction or position of the output beam depends on the wavelength [5,6]. An alternative design employs a Fabry-Pérot etalon as wavelength discriminator, operating in transmission [7]. In that case the two tasks of wavelength selection and feedback reflection are carried-out by two different optical elements. The etalon can either be formed from a thin air gap between two glass plates or a single, thin ($\sim 30\mu\text{m}$) solid plate. Both solutions are costly, can be fragile and exhibit multiple resonances. Furthermore, we observe that the absorption of atmospheric water can shift the transmitted wavelength to the point of uselessness after two years.

Better robustness and unique transmission is provided by narrow-band dielectric interference filters. Their use in an extended cavity laser has been demonstrated for telecom wavelength in [4]. The emission from the anti-reflection coated back facet of a $\lambda = 1300$ nm laser diode is fed-back by a "cat's eye" (lens + mirror). An interference filter of 2 nm passband width and 70 % peak transmission acts as intra-cavity wavelength discriminator.

Here, we present filters having 90 % transmission and ~ 0.3 nm FWHM at near infra-red and visible wavelengths. The external cavity is added to the output beam, while the diode's back facet is coated for high reflectivity. The cavity outcoupler is a partially reflecting mirror. Changing its reflectivity is an easy way of optimizing the feed-back. The diode's output facet has no particular high-quality anti-reflection coating giving rise to a second cavity formed by the laser chip itself, but making it inexpensive. Chaotic coupling to adjacent chip modes is efficiently suppressed by the narrow bandwidth of our filter, up to 8 times the threshold current.

We show that the sensitivity of these lasers to environmental perturbations is drastically reduced as compared to the Littrow configuration. We demonstrate tunability over a broader wavelength range thanks to the possibility of optimizing the amount of feedback independently from the wavelength selection mechanism. We study the lasers' spectral noise.

2 The external cavity

A schematic of the external cavity is given in Fig. 1. The light emitted from the diode (DL) is collimated by an objective lens (LC) with short focal length (3 to 4.5 mm) and high numerical aperture (~ 0.6). The lens is chosen to compensate for aberrations arising from the diode's packaging window. A partially reflecting mirror, here named out-coupler (OC) provides the feedback into the diode. The OC is displaced by a piezo-electric transducer (PZT) in order to vary the cavity length. A narrow-band high-transmission interference filter (FI) is introduced into the cavity. The filter provides the frequency selectivity

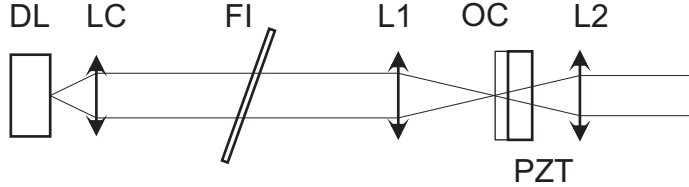


Fig. 1. Schematic of the external cavity laser using an interference filter (FI) for wavelength selection: (DL) laser diode, (LC) collimating lens, (OC) partially reflective out-coupler, (PZT) piezoelectric transducer actuating OC, (L1) lens forming a "cat's eye" with OC, (L2) lens providing a collimated output beam.

usually obtained by replacing the out-coupler with a diffraction grating. With this set-up, we are able to achieve single-mode, tunable operation. In addition much better stability against optical misalignment is achieved by focussing the collimated beam in a "cat's eye" onto the out-coupler. We typically employ a lens (L1) of 18 mm focal length. A second, similar lens (L2) provides a collimated output beam. Contrary to the Littrow laser design, reflection and wavelength discrimination are provided by two different elements so that the amount of feedback can easily be optimized.

In Fig. 1 the diode's back facet is coated for high reflection. Alternatively, this facet can have low reflection to provide the output beam. In that case one chooses OC with maximum reflectivity.

3 Tunability and wavelength sensitivity

For a Littrow laser wavelength discrimination is given by the Bragg condition $\lambda = 2d \sin \theta$ where d is the grating's line spacing and θ the angle of incidence. For wavelengths in the near infra-red, typical values are $d^{-1} = 1200$ lines/mm and $\theta = 30^\circ$. This leads to $d\lambda/d\theta \approx 1.4$ nm/mrad. Tuning the laser redirects the output beam by $2(d\lambda/d\theta)^{-1} \approx 1.4$ mrad/nm or, if a mirror is attached to the grating mount[6], leads to a transverse displacement of $dx/d\lambda = 18 \mu\text{m}/\text{nm}$ (assuming a distance of 15 mm between the grating and the mirror).

Wavelength discrimination of our filter is based on multiple reflection within its dielectric coatings and behaves as a thin Fabry-Pérot etalon with effective index of refraction n_{eff} . The transmitted wavelength is given by

$$\lambda = \lambda_{max} \sqrt{1 - \frac{\sin^2 \theta}{n_{eff}^2}} \quad (1)$$

where θ is again the angle of incidence. λ_{max} is the wavelength at normal incidence. A typical value is $n_{eff} = 2$ (see section 5). We choose the nominal wavelength to be transmitted at 6° of incidence which, for $\lambda_{max} = 853$ nm

leads to

$$\frac{d\lambda}{d\theta} = -23 \text{ pm/mrad.} \quad (2)$$

This is 60 times smaller than for the Littrow configuration. The corresponding reduction of the sensitivity of the wavelength against mechanical instabilities is a clear advantage of our design. Note that this reduction is not achieved at the expense of a reduced tunability (see section 7). Tuning the filter displaces the output beam by

$$\frac{dx}{d\lambda} = 8 \text{ } \mu\text{m/nm,} \quad (3)$$

due to the 0.5 mm thick fused-silica filter substrate ($n \sim 1.45$). This is two times smaller than for the modified Littrow laser. Note that if one chooses to out-couple from the diode's back facet, the displacement is further reduced.

4 Sensitivity of the optical feedback

We now study the sensitivity of the laser to a misalignment of the external cavity that does not affect the emission wavelength but the optical feedback. We consider a Gaussian beam with electric field E_{do} being emitted from the output facet of the diode ($z = 0$). Its propagation through the external cavity (along z) can be modeled in the paraxial approximation giving the reflected electric field E_{dr} at the output facet of the diode. The feedback $F = R^{-1} |\iint E_{do}^* E_{dr} dx dy|^2$ is given by the overlap integral of the reflected and emitted electric fields. For convenience we normalize by the reflectivity R of the grating/out-coupler. The variation of F under misalignment reflects the mechanical and thermal sensitivity of the laser.

Two sources of misalignment are considered: tilt of the out-coupler (grating) and axial displacement of the out-coupler. Displacements of other optical elements can be transformed into one of these. The computation of F turns out to be independent of the number of lenses in the cavity, and can be simplified by calculating the overlap integral $F = R^{-1} |\iint E_{rei}^* E_{rer} dx dy|^2$ at the position $z = z_{re}$ of the reflective element [4]. Here E_{rei} and E_{rer} are respectively the incident and reflected electric fields on the out-coupler. We assume that the incident beam is perfectly aligned so that it forms a waist of $1/e^2$ radius w_0 on the out-coupler.

If α is the angle formed by the incident and reflected beam due to a small tilt of the out-coupler, we find [4]

$$F = \exp \left[-(\alpha\pi w_0/\lambda)^2 \right] \quad (4)$$

and for $\alpha \rightarrow 0$

$$\frac{\partial^2 F}{\partial \alpha^2} = -\frac{2\pi^2 w_0^2}{\lambda^2} \quad (5)$$

Note that $\xi = \lambda/(\pi w_0)$ is the $1/e$ divergence angle.

On the other hand, if the reflective element is displaced along the optical axis by δ , the reflected beam has a radius of curvature $r = 2\delta + z_R^2/(2\delta)$ and $1/e^2$ radius $w = w_0\sqrt{1 + (z_R/(2\delta))^2}$ with Rayleigh length $z_R = \pi w_0^2/\lambda$. This gives

$$F = \left(1 + \frac{\delta^2 \lambda^2}{\pi^2 w_0^4}\right)^{-1} \quad (6)$$

and for $\delta \rightarrow 0$

$$\frac{\partial^2 F}{\partial \delta^2} = -\frac{2\lambda^2}{\pi^2 w_0^4} \quad (7)$$

Equations 5 and 7 show that w_0 is the only parameter which determines the sensitivity of the optical feedback to misalignment. In grating-tuned extended cavity lasers, the beam waist is essentially determined by the selectivity requirement and is of the order of 1 mm. This leads to a rather poor trade-off between angular and displacement sensitivity. Indeed, a tilt of the grating of $\alpha = 100 \mu\text{rad}$ is sufficient to decrease the coupling factor F by 10%, while a similar reduction due to a pure displacement would correspond to $\delta = 1$ m. In the new scheme described here the separation of the wavelength selection and optical feedback allows to choose a more favorable value for w_0 . In our cat's eye setup $w_0 \sim 10 \mu\text{m}$. Hence, the tilt or displacement reducing F by 10% ($\alpha = 9 \text{ mrad}$ or $\delta = 0.1 \text{ mm}$ respectively) are both very large deformations.

5 The filter

The interference filter [8] is formed of a series of dielectric coatings on an optical substrate with anti-reflection coated back face. It is calculated to transmit more than 90% of the intensity at the nominal wavelength at 6° incidence. The fullwidth at half maximum (FWHM) of the transmission curve is chosen as 0.3 nm, which is about twice the mode spacing of a typical laser diode. Filters with even higher finesse can be produced only at the cost of reduced transmission. The chosen compromise turns out to provide sufficient discrimination for stable single mode lasing with satisfactory output power (see section 6).

The samples tested here are fabricated on larger optical wafers and then cut into pieces of $5 \times 5 \text{ mm}^2$, thereby reducing the production costs. We test several fabrication batches at 698, 780 and 852 nm nominal wavelength. In the

following the measurements on a 852 nm filter are described. Similar results are obtained for the other wavelengths.

The transmission of a 1.2 mm diameter collimated beam of known wavelength is measured. Fig. 2 shows the results as a function of the angle of incidence for a 852.1 nm beam (\bullet) and a 843.9 nm beam (\circ). The first maximum has 89 % transmission at $\theta = 6.96(4)^\circ$ and a FWHM of $0.80(1)^\circ$. The 843.9 nm light is transmitted to 84 % at $\theta = 17.34^\circ$ with a FWHM of 0.40° . Using equation 1 we fit $\lambda_{max} = 853.7$ nm and $n_{eff} = 1.97$. This leads to $\Delta\lambda_{FWHM} = 0.37$ nm for 852 nm and $\Delta\lambda_{FWHM} = 0.44$ nm for 844 nm. The transmission peaks are well fitted by a Lorentzian taking the wavelength as argument. If the filter is used at a wavelength 8 nm below its nominal value the transmission drops by 5 % only. Repeating the measurement on 6 different production batches, we find less than 5 % variation of the maximum transmission at 852.1 nm.

In a second set of measurements, the transmission at 852.1 nm is determined as a function of the incident polarization. A sinusoidal variation from 89 % to 75 % is observed when the linear polarization rotates from parallel to perpendicular with respect to the axis of inclination.

Thirdly, the transmission is analyzed as a function of the position on the filter (Fig. 3). A 0.5 mm wide slit is placed in the 852.1 nm beam. Having optimized the angle of incidence at the center and keeping it fixed (\circ), the right half of the filter shows good homogeneous transmission, whereas the transmission drops drastically towards the left edge. When the angle of incidence is optimized at each position (\bullet), the transmission can be recovered to > 70 %. The corresponding angle at the left edge is 0.6 mrad bigger than the optimum angle at the center. Fig. 3 represents a batch with good spatial homogeneity. Stronger variations are observed for other samples. This result indicates that smaller beam diameters (< 1 mm) are favorable.

Finally we test the filters under vacuum. At a residual pressure of 10^{-4} Pa, we do not observe any variation of the optimal angle of transmission compared to atmospheric pressure to within our experimental resolution (5 GHz when expressed in terms of frequency). To ensure that desorption of residual gas from the coatings does not influence this result, the vacuum is kept over one month. This makes the filter a perfectly suited candidate for wavelength selection in space-born lasers.

6 A prototype emitting at 852 nm

Following the design of Fig. 1, a laser at 852 nm is built. The diode (SDL 5422) nominally emits 150 mW for a current of $I = 150$ mA at 854 nm.

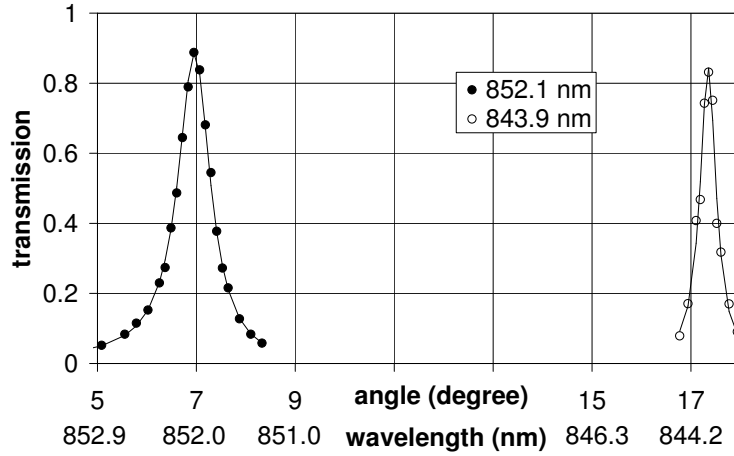


Fig. 2. Filter transmission of 852.1 nm light (●) and 843.9 nm light (○), as a function of the angle of incidence. The solid lines are Lorentzian fits to each peak.

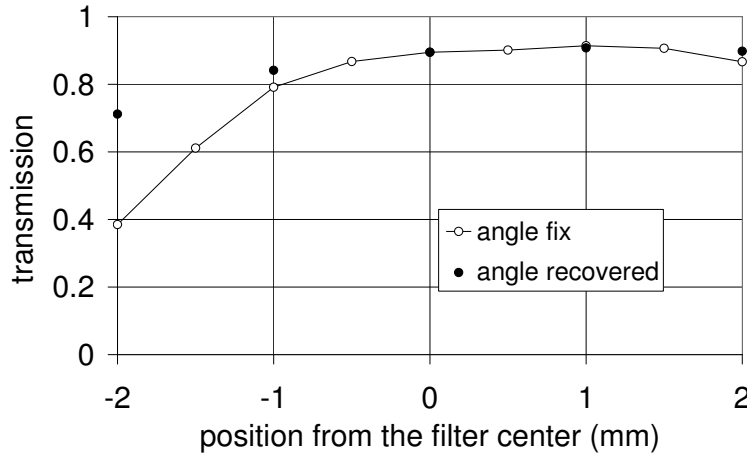


Fig. 3. Transmission of the 852 nm filter vs. position. When the angle of incidence is kept constant, the transmission drops at the left edge. If the angle is optimized at each point, it can be recovered to $> 70\%$.

The output facet coating is specified to induce less than 4 % reflection. We measure the free spectral range of the naked diode as ~ 50 GHz (0.13 nm), which corresponds to a physical length of ~ 0.8 mm assuming the index of refraction of GaAs ($n = 3.6$) [9].

The collimating lens has a focal length of 4.5 mm. L1 and L2 have focal length $f = 18.5$ and 11 mm, respectively. The out-coupler is an optical flat of 10 mm

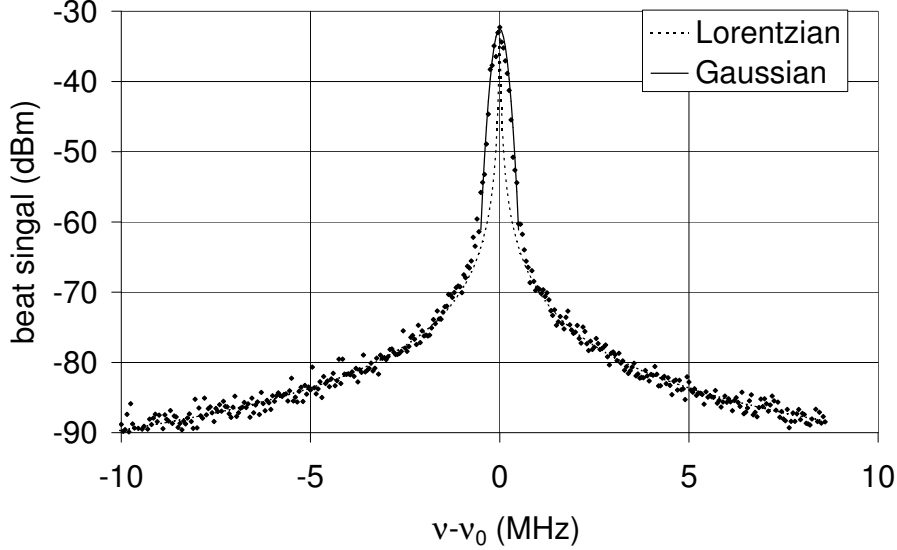


Fig. 4. Power spectrum of the beat signal at $\nu_0 = 8.75$ GHz between two identical 852 nm lasers. The solid line is a Gaussian fit to the central peak, the dashed line a Lorentzian fit to the wings. The spectrum analyzer’s resolution bandwidth is set to 1 kHz. The full trace is swept in 25 s.

diameter and 3 mm thickness. It is coated partially reflective on the inner face and anti-reflection on the outer. It is glued onto a 10 mm diameter PZT tube of 1 mm wall thickness and 10 mm length. The overall length of the external cavity is 70 mm.

Different reflection coefficients of the OC are tried. The output power at $I = 85$ mA is 47, 40 and 30 mW for 15, 20 and 30 % reflectivity, respectively. At 15 and 20 % reflection, single mode operation is obtained for certain intervals of the diode current only. At 30 % reflection stable single mode lasing is assured from the threshold current (~ 10 mA) to 8 times its value. Operation on the same diode mode is assured within a span of 4 mrad of filter inclination (44 GHz), before an adjacent mode of the diode is selected. This demonstrates the small sensitivity of our design to a tilt of the selective element (equation 2).

In order to determine the laser’s spectral properties, we measure the beat signal between two identical set-ups separated in frequency by $\nu_0 = 8.75$ GHz. The observed spectrum is shown in Fig. 4. The first laser is locked to the D2 line of Cs. The second one is locked (with a bandwidth of 15 kHz) to the first one so that the beat frequency stays constant. The remaining higher frequency noise leads to a random distribution of the central beat frequency, which is

well fitted by a Gaussian (solid line). We fit the points within ± 0.5 MHz from the center and find a FWHM of 155 kHz. The wings ($|\nu - \nu_0| > 1$ MHz) of the beat signal can be fitted by a Lorentzian (dashed line) giving the high frequency noise of the laser. Its FWHM of 28 kHz indicates that the white noise level of each laser corresponds to a linewidth of 14 kHz. An even smaller white noise floor may be obtained by means of stronger optical feedback or a longer external cavity.

Because of the filter's vacuum compatibility and the mechanical stability of our prototype, the design of Fig. 1 has been selected for the construction of space-qualified lasers for the PHARAO project [10]. Space qualification includes survival in vibratory environments with sinusoidal excitation (30 Hz) at a level of $\pm 35 g$ during 120 s and random excitation (20-600 Hz) with a level of 31 g rms during 120 s. The qualification model has passed the vibration tests. Its spectral characteristics did not change and the output beam mis-orientation remained below 10 μrad .

Using a *Sharp* diode (GH0781JA2C) and a 780 nm filter in a similar external cavity we generate laser light for the manipulation of atomic rubidium.

7 A prototype emitting at 698 nm

Similar components are used to build a laser at 698 nm with a 100 mm long external cavity. A *CircuLaser* diode (PS 107) specified at 688 nm is used. Its free running output power is 30 mW for $I = 100$ mA at room temperature. The interference filter used here is specified for 698 nm at 6° of incidence. The measured optimal incidence is 9° . By varying the inclination of the filter, the temperature of the diode and the reflection coefficient of the OC, we achieve lasing from 679 nm to 700 nm with the same non AR-coated diode. Emission at 679 nm is easily obtained by using a 40 % reflection OC and cooling the diode to 19°C . The output power is 4 mW, for $I = 60$ mA. Even smaller wavelengths seem reachable, only limited by the size of the filter mount. It is more difficult to reach 698 nm, as this wavelength lies at the very edge of the diode's gain curve. We heat the diode to 40°C . 60 % reflectivity of the OC gives stable single mode lasing but limited output power. 50 % reflection leads to an output power of 2 mW at $I = 57$ mA with sufficient mode selection. No emission at 698 nm is observed for 40 % reflection. Finally, due to operation at the very edge of the gain curve, the possibility to tune the laser by varying the current of the diode laser is limited to 40 GHz, as compared to 70 GHz if the diode is emitting at its nominal wavelength.

The tunability of this laser is significantly larger than we had formerly achieved with grating feedback. This may be due to the fact that the coupling of the

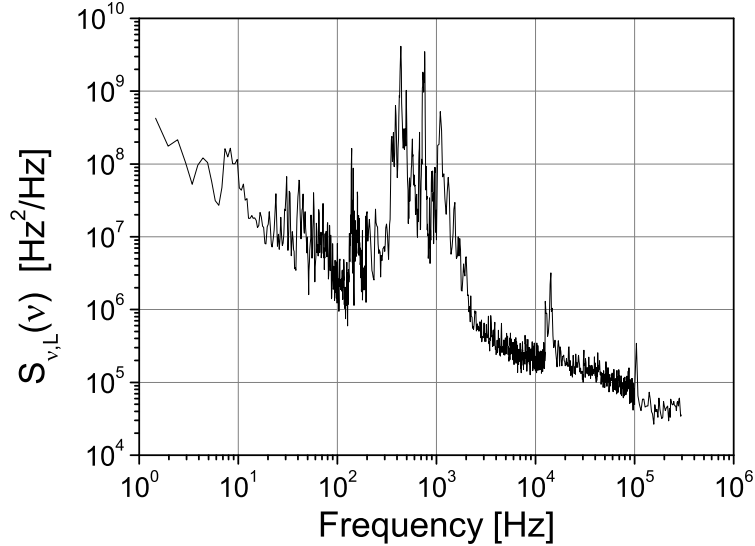


Fig. 5. Power spectral density of frequency fluctuations of the 698 nm prototype.

diode to the external cavity is more easily optimized with the design of figure 1. In addition, the grating induces aberrations which are difficult to compensate for. Being able to pull the diodes more than 10 nm away from their nominal wavelength is another advantage of the new setup, especially in spectral regions where laser diodes are not available, like 700 nm.

We measure the frequency noise of the interference filter laser against a 400 mm long Fabry-Pérot cavity of finesse 300. Both, the laser and the cavity are free running. The observed frequency noise power spectral density $S_{\nu,L}(\nu)$ is plotted in Fig. 5. From 2 Hz to 300 kHz, $S_{\nu,L}(\nu)$ essentially decreases with $1/\nu$ corresponding to flicker frequency noise. Peaks due to acoustic perturbations are also observed for Fourier frequencies between 100 Hz and 2 kHz. From Fig. 5 we can deduce the fast linewidth $\Delta\nu_L$ of the laser using [11]

$$\int_{\Delta\nu_L/2}^{\infty} S_{\phi,L}(\nu) d\nu = \frac{2}{\pi} \quad (8)$$

where $S_{\phi,L} = S_{\nu,L}/\nu^2$ is the power spectral density of phase fluctuations. We find a fast linewidth $\Delta\nu_L = 150$ kHz.

8 Conclusion

We have built external cavity diode lasers using an interference filter as wavelength selective element. The filter presents high transmission and narrow bandwidth. The cavity design drastically improves the laser's passive stability and reduces beam walk when tuned. The amount of feedback can easily be

varied by the reflectivity of the out-coupler. Prototypes at different wavelength in the visible and near infra-red were realized showing a linewidth down to 14 kHz. Tuning over 20 nm was demonstrated. The prototypes are currently employed in atomic physics experiments on Cs, Rb and Sr, e.g. for laser cooling.

Acknowledgements

We are grateful to A. Landragin for fruitful discussion.

References

- [*] Unité de Recherche de l'Observatoire de Paris et de l'Université Pierre et Marie Curie associée au CNRS, laboratoire national de métrologie du Laboratoire National de Métrologie et d'Essais
- [1] C.E. Wieman and L. Hollberg, "Using diode lasers for atomic physics", *Rev. Sci. Instrum.* **62**, 1-20 (1991).
- [2] M.W. Flemming and A. Mooradian, "Spectral characteristics of external-cavity controlled semiconductor lasers", *IEEE J. Quantum Electron.* **17**, 44-59 (1981)
- [3] Since a grating selects the wavelength in air, passing from ambient pressure to vacuum changes the index of refraction by 3×10^{-4} corresponding to $\Delta\lambda = 0.26$ nm (100 GHz) at $\lambda = 852$ nm.
- [4] P. Zorabedian and W.R. Trutna Jr., "Interference-filter-tuned, alignment-stabilized, semiconductor external-cavity laser", *Opt. Lett.* **13**, 826-828 (1988)
- [5] L. Ricci, M. Weidemüller, T. Esslinger, A. Hemmerich, C. Zimmermann, V. Vuletic, W. König, and T. W. Hänsch, "A compact grating-stabilized diode laser system for atomic physics", *Opt. Commun.* **117**, 541-549 (1995).
- [6] C.J. Hawthron *et al*, "Littrow configuration tunable external cavity diode laser with fixed direction output beam", *Rev. Sci. Instrum.* **72**, 4477-4479 (2001)
- [7] F. Allard *et al*, "Automatic system to control the operation of an extended cavity diode laser", *Rev. Sci. Instrum.* **75**, 54-58 (2004)
- [8] fabricated by Research Electro-Optics Inc., Boulder, USA
- [9] A.E. Siegmann, *Lasers* (University Science Books, Sausalito, 1986).
- [10] C. Salomon *et al*, "Cold atoms in space and atomic clocks : ACES : Missions spatiales en physique fondamentale", *C. R. Acad. Sci. Serie-IV* **2** (9), 1313-1330 (2001).

- [11] D. Halford, "Infrared microwave frequency synthesis design, some relevant conceptual noise aspects", in *Frequency Standards Metrology Seminar*, (Laval, Quebec, 1971), pp. 431-466